Soft Matter

PAPER

View Article Online
View Journal | View Issue

Cite this: *Soft Matter*, 2018, **14**, 3748

Influence of dielectric inhomogeneities on the structure of charged nanoparticles in neutral polymer solutions†

Rituparna Samanta and Venkat Ganesan *

Received 9th February 2018,
Accepted 17th April 2018

DOI: 10.1039/c8sm00298c

rsc.li/soft-matter-journal

We study the structural characteristics of a system of charged nanoparticles in a neutral polymer solution while accounting for the differences in the dielectric constant between the particles, polymer and the solvent. We use a hybrid computational methodology involving a combination of single chain in mean-field simulations and the solution of the Poisson's equation for the electrostatic field. We quantify the resulting particle structural features in terms of radial distribution function among particles as a function of the dielectric contrast, particle charge, particle volume fraction and polymer concentration. In the absence of polymers, charged macroions experience increased repulsion with a lowering of the ratio of particle to solvent dielectric constant. The influence of the dielectric contrast between the particle and the solvent however diminishes with an increase in the particle volume fraction and/or its charge. In the presence of neutral polymers, similar effects manifest, but with the additional physics arising from the fact that the polymer-induced interactions are influenced by the dielectric contrast of the particle and solvent.

1 Introduction

Nanoclusters formed during aggregation of charged metal particles and proteins in the presence of polymers constitute the basis of many applications like bio-imaging, catalysis, drug delivery *etc.*[1–4] The structure and phase behaviors that manifest in such systems are understood as a consequence of the interplay between the electrostatics and the polymer-mediated interactions.[5–7] While many previous studies of such systems have addressed the influence of electrostatic interactions on the resulting phase behavior,[8–12] in most models, the dielectric constant of the particle is assumed to be identical to that of the solvent. However, the influence of dielectric contrast (between the particle and the solvent) may become crucial in some situations, especially, in aqueous solutions where the proteins and nanoparticles are often characterized by dielectric constants of the order of $\approx$2.0–8.0 (relative to that of vacuum), whereas that for solvent (water) is of the order of $\approx$80.0 in same units.[13–19] Moreover, when the particles are present in a polymer solution, the dielectric constant of the polymer is also expected to influence the electrostatic and the polymer-mediated interactions. To our knowledge, there has not been any study examining the influence of such dielectric contrast(s) on the structure of particle suspensions in polymer solutions.

A few earlier studies have addressed the influence of particle–solvent dielectric contrast on the electrostatic interactions in the system of one or two charged particles in solvent.[13,16,17,20–25] For instance, Messina[17] presented the results for image force and counterion distributions around the spherical macroions in both salt and salt free environments. In other work,[16] Linse presented expressions for the polarized surface charge, potential energy for arbitrary number of electrostatic multipoles localized in spherical cavities. Such studies have demonstrated when the dielectric constant of the particle is lower (higher) than the solvent, the sign of induced polarized charge is same (opposite) as that of the ion, thereby resulting in an additional repulsive (attractive) interaction between the particles.[13–17,26]

In contrast to the situation of charged particles in simple electrolytes, there is comparatively less number of studies when the macroions are in a neutral polymer solution. In a recent work from our group,[27,28] polymer Self Consistent Field Theory (SCFT) was used to study the polymer-mediated interparticle interactions between two spherically charged bodies in polyelectrolyte solutions. We considered the case where the dielectric constant of both the particle and polymers are lower than that of the solvent, and demonstrated that similar to the situation of simple electrolytes there is an enhancement of interparticle repulsive interaction arising from the image charges of counterions, oppositely charged polymers and the other particle.

Department of Chemical Engineering, University of Texas at Austin, Austin, Texas 78712, USA. E-mail: venkat@che.utexas.edu

† Electronic supplementary information (ESI) available. See DOI: 10.1039/c8sm00298c

While the above studies have contributed useful insights, there are much less studies dealing with the physics of multiparticle systems.[13–17,26,29] For instance, Barros *et al.* studied the effect of inhomogeneous dielectric constant on self-assembly of a mixture of charged colloids of different charge and sizes.[18] For the system with dielectric constant ratios of particle to solvent greater than unity, they observed unique string like particle arrangements arising from image charge effects. Whereas, for particle–solvent dielectric ratio less than unity, they observed self-assembled structures similar to NaCl. Recently Qin *et al.*[19,30] developed an analytical approach to calculate polarization energy for a multiple charged particle system in a medium with different dielectric constant. Their study demonstrated that the polarization effects alter the structural behavior, and can lead to the formation of higher order structures which do not manifest in the absence of dielectric contrast.

In a recent work from our group, Pandav *et al.*[11] developed a multiparticle simulation framework to study the structure and phase of mixtures of charged nanoparticles and neutral/charged polymers. Such an approach avoids any assumption about the applicability of pairwise polymer-mediated interparticle potentials, and instead accounts for the full multibody nature of polymer-mediated interactions. In such a context, we demonstrated that even for dilute particle concentrations, the pairwise polymer-mediated interactions deduced in the infinite dilute limit of particle concentration over-predicts particle aggregation relative to the multibody framework. Although our study considered multibody effects and electrostatic interactions, the dielectric constant of the particles was assumed to be same as that of the solvent, and hence the interplay of multibody effects and electrostatic screening due to dielectric inhomogeneity was unexplored.[11]

To summarize, the above discussion illustrates that there is a relative lack of understanding of the influence of polymerization effects and the interplay with depletion interactions for multiparticle systems. Motivated by such issues, in this work we aim to extend the methodology of Pandav *et al.* to address the physics of such situations.[11] Explicitly, we extend our multibody framework to study the influence of the dielectric inhomogeneity on the structural characteristics of charged particles in neutral polymer solutions. We focus on the nanoparticle regime where the radius of particle is of the same order as the radius of gyration of homopolymer. In such a regime, we quantify the manner by which particle concentration, charge of the particles, concentration of polymers and valency of counterions influence the particle structural characteristics in systems where the particle and polymer dielectric constants are different from that of the solvent.

The rest of the article is organized as follows. In Section 2 we discuss the model details underlying the simulation methodology. In Section 3, we discuss the parameters and numerical methodologies used for the simulation framework. In Section 4 we present results for the structural properties of a system of charged particles in solution (System I) interacting through pairwise LJ attractions. Subsequently, we discuss the results for the case when polymers are present (System II) in the solution, which induces an attractive depletion interaction between particles. We conclude the article with a summary of results and findings in Section 5.

2 Model description

In this work, we have studied two related classes of systems. In the first system (addressed as System I hereafter), we study the effect of dielectric inhomogeneity on the structure in a system of charged spherical particles in an electrolyte solvent. In this case, the particles are assumed to interact by pairwise LJ interactions. Our proposal is to use such a model to understand the physics of electrostatic interactions in multiparticle colloidal electrolyte systems when the dielectric constant of the particles are less than that of the solvent. The second system (System II) considers charged nanoparticles in an uncharged polymer solution. Therein, we address the physics of interplay between electrostatic and depletion interactions.

In this study, we consider a system of N_p charged spherical particles of radius R_p in presence of an implicit solvent in a periodic cubic box of volume V. For System II, we also include n uncharged polymer chains of m monomers each of radius of gyration R_g. We denote the total charge on each particle by Q_p. We assume that the charge of the particle is uniformly distributed over the volume of the particle such that all the grid points covering the volume of the particle has a fractional charge z_p. To maintain overall electroneutrality of the system, n_c point counterions of the charged particles are also included. The concentration of the polymer is presented in units of the overlap concentration C^* of an ideal linear polymer chain solution. The volume fraction of particles is denoted as ϕ_p. The dielectric constant of the particle is denoted as ε_p and that of the solvent as ε_w. In cases where the polymers are included (System II), the polymer dielectric constant is assumed to be identical to ε_p. For System II, the intramolecular interactions in the polymer chains are modeled through a bead spring model, with bonded Hookean interactions between the beads:

$$\frac{H_b}{k_B T} = \frac{3}{2b^2}\sum_{i=1}^{n}\sum_{s=1}^{m-1}[\mathbf{r}_i(s) - \mathbf{r}_i(s+1)]^2 \quad (1)$$

where $r_i(s)$ represents the coordinate of the sth bead on the ith polymer. A model of excluded volume interactions between the polymer segments is incorporated through a simplistic implicit solvent interaction potential of the form:

$$\frac{\bar{u}(\mathbf{r})}{k_B T} = u_0\delta(\mathbf{r}) \quad (2)$$

where u_0 is commonly known as the excluded volume parameter.[31] For this study, we have used a value $u_0 = 10$ representing a good solvent.

In the above framework, the nonbonded interaction between the polymer segments can be formally represented as:

$$\frac{H_s}{k_B T} = \frac{u_0}{2}\int \hat{\rho}_{poly}{}^2(\mathbf{r})\mathrm{d}\mathbf{r} \quad (3)$$

where $\hat{\rho}_{\text{poly}}$ is the microscopic polymer segment density,[32]

$$\hat{\rho}_{\text{poly}}(\mathbf{r}) = \sum_{i=1}^{n}\sum_{s=1}^{m}\delta(\mathbf{r} - \mathbf{r}_i(s)). \quad (4)$$

The instantaneous density of particles is similarly quantified through a particle volume fraction field as:

$$\rho_{\text{part}}(\mathbf{r}) = \sum_{i=1}^{N_p}\int_{r_i}^{r_i+R_p}\hat{\rho}_{\text{part}}(\mathbf{r})h(|\mathbf{r}' - \mathbf{r}_i|)\mathrm{d}\mathbf{r}' \quad (5)$$

where $\hat{\rho}_{\text{part}}(\mathbf{r}) = \delta(\mathbf{r} - \mathbf{r}_i)$ and $h(r) = 1$ where $|r| < R_p$. The ions in the simulation are considered to be point charges and their microscopic densities are given by:

$$\rho_{\text{ion}}(\mathbf{r}) = \sum_{i=1}^{n_c}\delta(\mathbf{r} - \mathbf{r}_i). \quad (6)$$

For modeling the particle–counterion interactions, the particles are envisioned as spherical particle with a thin layer of penetrable soft core surrounding an impenetrable hard core. The repulsive interaction between the particle and the polymer monomers, counterions are modeled through a potential of the form:

$$W_{\text{cp}}(\mathbf{r}) = 50\left[1 - \tanh\left(2\frac{\mathbf{r} - \alpha R_p}{\beta}\right)\right]k_B T. \quad (7)$$

The coefficients α,β control the steepness and range over which the potential decays from $100k_BT$ to $0k_BT$. We have used $\alpha = 0.9$ and $\beta = 0.5$ for the simulation, which ensures that the particle cores are almost impenetrable to counterions and polymers.

In general, interparticle interactions are modeled as follows:

$$\frac{H_{\text{pp}}}{k_B T} = \frac{1}{2}\sum_{i=1}^{N_p}\sum_{j=1(j\neq i)}^{N_p}U(|\mathbf{r} - \mathbf{r}'|) \quad (8)$$

For the situation in which polymers are not considered in our model (System I), U is modeled as a Lennard Jonnes potential of the form:

$$U_{\text{LJ}}(r) = 4\varepsilon_{\text{LJ}}\left[\left(\frac{\sigma}{r}\right)^{12} - \left(\frac{\sigma}{r}\right)^{6}\right] \quad (9)$$

where r is the center to center interparticle distance and $\varepsilon_{\text{LJ}} = 0.1k_BT$ throughout the study. For System II, when polymers are introduced, U is modeled as a hard sphere interaction U_{HS}:

$$U_{\text{HS}}(r) = \begin{cases} 0, & \text{if } r \geq 2R_p \\ \infty, & \text{if } r < 2R_p. \end{cases} \quad (10)$$

For our study we have used the Single Chain in Mean Field (SCMF) approach introduced by Mueller and coworkers.[33] In the SCMF framework, the non-bonded pair-wise interactions are replaced with fluctuating potential fields which are conjugate to the corresponding density fields. The expressions for such fields can be obtained by the saddle point approximation of the corresponding field theory.[33] The electrostatic energy arising from the charges is given as:

$$\frac{H_{\text{el}}}{k_B T} = \int\mathrm{d}\mathbf{r}\left[\rho_e(\mathbf{r})\varphi(\mathbf{r}) - \frac{\varepsilon(\mathbf{r})}{\varepsilon_w}\frac{1}{8\pi l_b}|\nabla\varphi(\mathbf{r})|^2\right] \quad (11)$$

The electrostatic potential $\varphi(\mathbf{r})$, is in units of k_BT/e and is obtained as the solution of Poisson's equation

$$\nabla\cdot\left[\frac{\varepsilon(\mathbf{r})}{\varepsilon_w}\nabla\varphi(\mathbf{r})\right] = -(4\pi l_b)\rho_e(\mathbf{r}) \quad (12)$$

In the above, $\rho_e(\mathbf{r})$ is the charge density due to particle and counterions (in units of e), and is given as:

$$\rho_e(\mathbf{r}) = z_p\rho_{\text{part}}(\mathbf{r}) \pm \sum_{\text{ion}} z_{\text{ion}}\rho_{\text{ion}}(\mathbf{r}) \quad (13)$$

where z_{ion} is the valency of each ion (co- or counterions), z_p is the fractional charge of the particle and $\rho_{\text{ion}}(\mathbf{r})$ denotes the local density of co- and counterions.

In this work the local, inhomogeneous dielectric coefficient of the system is modeled using a simple functional form

$$\frac{\varepsilon(r)}{\varepsilon_w} = \left(1 + \left(\frac{\varepsilon_p}{\varepsilon_w} - 1\right)\rho_{\text{part}}(r) + \left(\frac{\varepsilon_{\text{poly}}}{\varepsilon_w} - 1\right)\frac{\rho_{\text{poly}}(r)}{C^{**}}\right) \quad (14)$$

where $\varepsilon(r)$ denotes the local dielectric constant in units of permittivity of vaccuum $\varepsilon_0 = 8.85 \times 10^{-12}$ ($C^2\ J^{-1}\ m^{-1}$) and C^{**} denotes the concentration of polymer melt. In the above, ε_w, ε_p, $\varepsilon_{\text{poly}}$ denote the relative dielectric constants of solvent, particle and polymer respectively. To keep the study simple, we do not consider the phenomenon of reduction of dielectric constant of water due to presence of other ionic species as is addressed in some of the advanced studies.[34–36]

3 Numerical methods and parameters

The model described above is used in a Monte Carlo simulation approach in which the configuration space is sampled using the Metropolis algorithm.[37] We began the simulation by placing the particles in a cubic lattice configuration and the polymers randomly in space. To render the simulations faster, an equilibrium distribution of counterions is assumed based on the electrostatic potential and the particle–counterion interaction potentials. The initial portion of the simulation involves 10^4 Monte Carlo (MC) moves in which only the polymers are moved while keeping the particles fixed in space. This pre-equilibration method is done to ensure removal of any particle–polymer overlaps. Subsequently, each Monte Carlo step (MCS) involves a MC move for all particles, a slithering snake move for all polymer chains and 150 MC moves for all polymers. Using such a sequence of moves, the system is equilibrated for 4.9×10^4 MCS (rendering the total equilibration cycle 5.9×10^4 MCS). Subsequently, the properties are averaged over 2×10^4 MCS, constituting the production cycle. Using the position of the monomers and particles, the density fields are updated after every move of the polymer and particles. The electrostatic potential $\varphi(\mathbf{r})$ is updated after every MCS (150 MC moves of the polymers) with the dielectric constant based on the averaged density of particle charge and counterions.

We use an iterative Fast Fourier Transform (FFT) based numerical method to solve the Poisson Boltzmann equation

(eqn (12)). Explicitly, the Poisson's equation defined in eqn (12) can be rearranged as follows:

$$\nabla \ln\left(\frac{\varepsilon(r)}{\varepsilon_w}\right)\cdot\nabla\varphi(r)+\nabla^2\varphi(r)=-4\pi l_b\frac{\varepsilon_w}{\varepsilon(r)}\rho_e(r) \quad (15)$$

To solve the above equation, we use a 2-step iterative procedure of the form (i denotes the step of iteration):

$$\varphi_{i+1}{}^{*}=\nabla^{-2}\left(-4\pi l_b\frac{\varepsilon_w}{\varepsilon(r)}\rho_e(r)-\nabla\ln\left(\frac{\varepsilon(r)}{\varepsilon_w}\right)\cdot\nabla\varphi_i\right) \quad (16)$$

$$\varphi_{i+1}=\lambda\varphi_i+(1-\lambda)\varphi_{i+1}{}^{*} \quad (17)$$

where ∇^{-2} denotes the inverse of the Laplacian operator and is calculated using Fast Fourier Transform (FFT). For our study, we have used the Bjerrum length (l_b) as 0.7 nm, corresponding to that of water at 300 K. The parameter λ is chosen between 0 to 1 to achieve convergence. In our simulations, we have used a value of λ = 0.30 and a convergence criterion:

$$\sqrt{\sum_{1}^{n_{total}}\left(\varphi_{i+1}-\varphi_i\right)^2}\le 0.001 \quad (18)$$

where n_{total} is the total number of grid points.

For the simulation, we have used a periodic cubic box of size 200 nm $\approx 10R_p\times 10R_p\times 10R_p$ divided into a $64\times64\times64$ grids. The specific choice of discretization was adopted by comparing the accuracy of the field arising from a point particle near a charged particle (Fig. S1 in the ESI†) with the analytic series solution for such a system in literature.[14] Moreover, we also verified our results for the particle structure against a finer grid of 128^3, and found very little quantitative differences between the results for the finer and coarser grid. The particles used in the simulation are of radii R_p = 20 nm and the homopolymers of R_g = 24 nm. In this study, we did not probe the effect varying R_p and R_g. The simulation is executed using an OpenMP FORTRAN program, compiled and run in a 24 core computer node. For a System I simulation at the lowest density ϕ_p = 0.188, the equillibration cycle (4.9×10^4 MCS) took approximately 3 hours for a homogeneous dielectric system and 4 hours for the inhomogeneous system.

4 Results and discussion

4.1 Structural characteristics of System I

In this section we present results for System I which considers charged particles in a solvent in the absence of polymers. The ratio of dielectric constant of the particle to that of the solvent ($\varepsilon_p/\varepsilon_w$) is used as a measure of the dielectric contrast, with the homogeneous case corresponding to $\varepsilon_p/\varepsilon_w$ = 1.0.

To set the context for understanding the influence of dielectric inhomogeneity between the particle and the solvent, we first briefly review some analytic results from previous studies.[14,17,38] The electrostatic interaction energy between a charged sphere of radius a with a net charge Q_p and a point charge q at a distance b from the center of the sphere is given as:

$$\frac{U_{sph}}{k_BT}=\frac{l_b}{b}\left[Q_pq+\frac{1}{2}\sum_{n=1}^{\infty}\left(\frac{a}{b}\right)^{(2n+1)}q^2\frac{(\varepsilon_w-\varepsilon_p)n}{\varepsilon_w(n+1)+\varepsilon_pn}\right]. \quad (19)$$

In the above expression, the first term represents the Coulomb interactions arising between the bare charges. The second term arises from the polarized charge on the particle due to the point charge q. Explicitly, when the ratio $\varepsilon_p/\varepsilon_w$, is lesser than 1.0, the polarized charge on the particle is of the same sign as q and the additional electrostatic energy is repulsive. In contrast, when the ratio $\varepsilon_p/\varepsilon_w$, is greater than 1.0, the polarized charge on the particle is of the opposite sign and thus the additional electrostatic energy is attractive. When the particle is uncharged, Q_p = 0, the electrostatic energy is:

$$\frac{U_{sph}}{k_BT}=\frac{l_b}{b}q^2\left[\frac{1}{2}\sum_{n=1}^{\infty}\left(\frac{a}{b}\right)^{(2n+1)}\frac{(\varepsilon_w-\varepsilon_p)n}{\varepsilon_w(n+1)+\varepsilon_pn}\right]. \quad (20)$$

The point charge induces a polarized surface charge (σ_p) density on the spherical particle:[17]

$$\sigma_p(\cos\theta)=\frac{q}{4\pi\varepsilon_wb^2}\sum_{n=1}^{\infty}\left(\frac{a}{b}\right)^{n-1}(2n+1)n\times\frac{(\varepsilon_w-\varepsilon_p)n}{\varepsilon_w(n+1)+\varepsilon_pn}P_n(\cos\theta) \quad (21)$$

where $P_n(\cos\theta)$ is the Legendre polynomial of order n, θ is the angle between lines joining a point r and b from the center (Fig. S2 in ESI†). The net charge due to polarization $Q=\int_{-1}^{1}2\pi a^2\sigma_p(\cos\theta)d\theta=0$, meaning there is no extra charge contribution from the polarized charge.[17]

In this study, we considered $\varepsilon_p/\varepsilon_w$ = 0.1 as a model for studying the dielectric inhomogeneity of protein/nanoparticle system in aqueous solutions.

4.1.1 Effect of counterion valency. In Fig. 1(a), we present results comparing the interparticle radial distribution function (RDF) at a specified particle volume fraction and charge for the system with dielectric contrast to the homogeneous system. For a specified counterion valency, we observe a lower peak in the particle–particle radial distribution function (RDF) for the system with dielectric inhomogeneities ($\varepsilon_p/\varepsilon_s<1.0$). Such results are indicative of a weaker aggregation tendency of the particles, signaling an enhancement in the effective repulsive interaction between the particles for the inhomogeneous dielectric cases.

To rationalize the above observations, we probed the normalized net counterion charge around a particle, $Q(r)$, defined as follows:

$$Q(r)=\frac{1}{Q_p}\int_{R_p}^{r}4\pi u^2z_{ion}\rho_{ion}du. \quad (22)$$

Such a measure enables us to quantify the screening of the particle charge by the counterions. From the results displayed in the Fig. 1(b), we observe that in the case when the dielectric constant of the particles is different from the solvent, the net charge of the counterions is less negative (relative to the homogeneous case), indicating that a lower density of counterions are

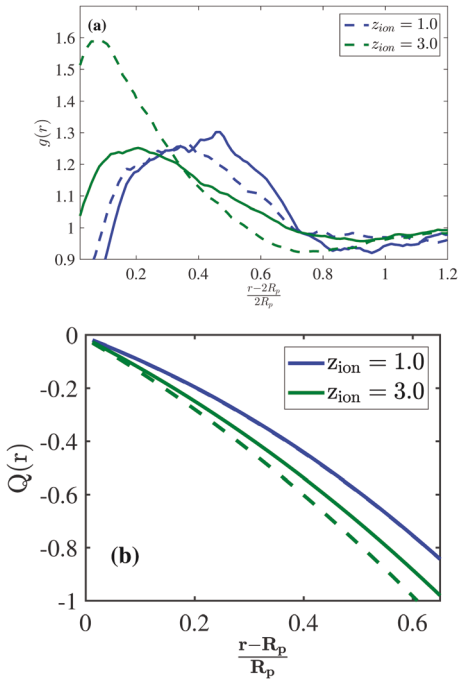

Fig. 1 (a) Particle–particle RDF for different dielectric constant of the particles at $\phi_p = 0.188$, $Q_p = 10$ and different counterion valencies $z_{ion} = 1, 3$; (b) average net counterion charge around particle. The dashed lines are for $\varepsilon_p/\varepsilon_w = 1.0$ and solid lines for $\varepsilon_p/\varepsilon_w = 0.1$.

present at a given distance from the center of the particle. To understand such results, we note that for the situation when dielectric constant of the particle is lesser than that of the solvent, the polarized charges corresponding to the counterions are expected to be of the same sign (eqn (19)) as the bare charge of the counterions. This gives rise to an additional effective repulsive interaction between particles and counterions. As seen in the Fig. 1(b), such a repulsion leads to a lower density of counterions $Q(r)$ screening the particle charge. As a consequence of this lower net charge $Q(r)$, the electrostatic interaction between the particles are expected to be less screened in systems with dielectric inhomogeneities, and thereby explains the trends manifested in the RDF (Fig. 1(a)).

In Fig. 1(a), we also observe that with increase in the counterion valency, the differences in the peak of RDF for the homogeneous and inhomogeneous systems, become more pronounced. Such results can also be rationalized as a consequence of differences in the screening of the electrostatic field in case of homogeneous and inhomogeneous dielectric constant system. As seen in Fig. 1(b), for $z_{ion} = 1.0$, at a distance $r \approx 0.4R_p$ from the surface of the sphere, the homogeneous and inhomogeneous cases compensate 42.82 and 43.00 percent of a net particle charge respectively. However, at the same distance, for $z_{ion} = 3.0$, the charge compensations are 53.06 and 60.01 percent of the net charge of the particle for homogeneous and inhomogeneous cases respectively. Such results indicate a stronger screening of the particle charges by the multivalent counterions. The origin of such trends can be traced to the fact that the potential energy due to the polarized charge is proportional to the square of the valency of counterion (eqn (19)).[17,38] Hence, the counterions with a higher valency are expected to induce a stronger polarized charge repelling the counterions from the particle surface. As a consequence of such reduced screening of the particle charge, the interparticle repulsion are expected to be enhanced and lead to the lower peak in the particle–particle RDF.

4.1.2 Effect of particle volume fraction. Fig. 2(a) displays the effect of particle volume fraction on the radial distribution function of particles (for a fixed particle charge $Q_p = 10$). For both homogeneous and inhomogeneous dielectric cases, the peak of particle–particle RDF is seen to increase with increase

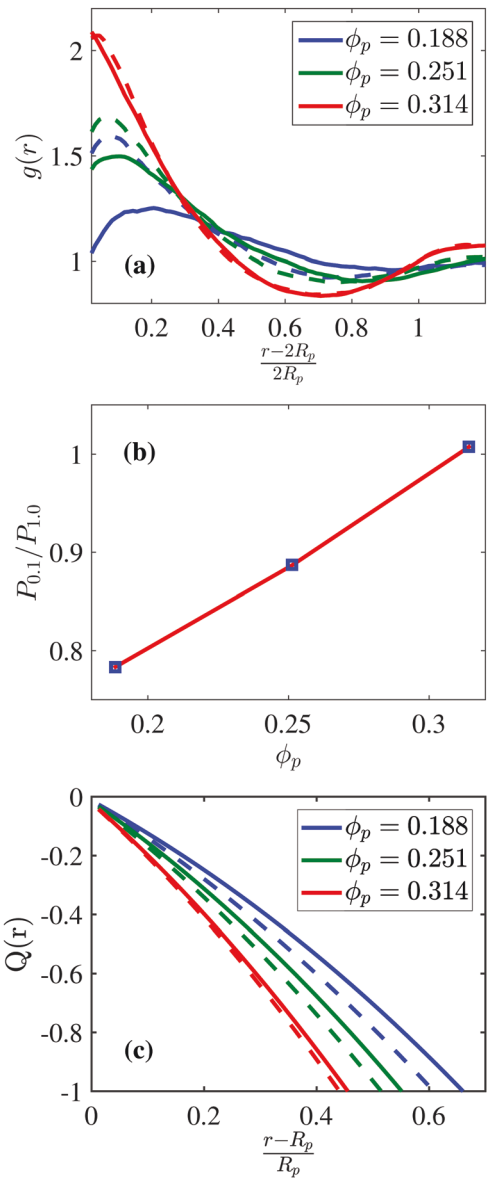

Fig. 2 (a) Particle–particle RDF at different dielectric constant at $Q_p = 10$, counterion valency $z_{ion} = 3.0$ and different particle volume fraction ϕ_p; (b) ratio of peaks of the RDF represented by P_1 and $P_{0.1}$ for $\varepsilon_p/\varepsilon_w = 1.0$ and $\varepsilon_p/\varepsilon_w = 0.1$ respectively. The line represents a guide to the eye. (c) Average net charge around particle. The dashed lines are for $\varepsilon_p/\varepsilon_w = 1.0$ and solid lines for $\varepsilon_p/\varepsilon_w = 0.1$.

in particle volume fraction, signaling a decrease in the effective electrostatic repulsion between the particles. Such an effect can be rationalized as a consequence of electrostatic screening arising from the other particles (Fig. 2(c)). Indeed, with increase in volume fraction of particles, the effective Debye screening length of the solution is expected to decrease. As a consequence, the effective particle–particle electrostatic interactions are expected to become weaker.[39]

Of more interest is the interplay between inhomogeneity of dielectric constant and the particle volume fraction. To quantify this effect, in Fig. 2(b), we present the ratio of peak values of particle–particle RDF for the cases $\varepsilon_p/\varepsilon_w = 0.1$ and $\varepsilon_p/\varepsilon_w = 1$ as a function of particle volume fraction. It can be seen that this ratio is always lesser than or equal to 1.0, indicating that the inhomogeneous dielectric system exhibit a stronger effective interparticle repulsion when compared with the homogeneous dielectric systems. Such a trend is consistent with the results and the accompanying discussion presented in Section 4.1.1. More interestingly, the relative peak value (Fig. 2(b)) is seen to increase (*i.e.* asymptotically approach 1.0) with an increase in the volume fraction of the particles. Such results indicate that the effect of dielectric inhomogeneity becomes mitigated at higher particle volume fractions.

To explain the above effect of dielectric inhomogeneity, we again turn to the net counterion charge distribution $Q(r)$ and its dependence on the dielectric contrast as a measure of polarization effects. In the results displayed in Fig. 2(c), we observe for all inhomogeneous dielectric cases, due to the effect of induced charges, less counterions are present near the particle surface when compared to the corresponding homogeneous cases. Such results are consistent with the discussion in the previous Section 4.1.1. More interestingly, we observe that at higher particle volume fractions, the differences in $Q(r)$ between the homogeneous and inhomogeneous systems become reduced. The multibody effect on such particle-induced polarization effects may also contribute to such results.

In an earlier work,[16,40] Linse considered the structure of three similar charged particles (with different dielectric constant than the solvent) arranged collinearly, and showed that there is a cancellation of the electric fields originating from the two outer particles on the central particle, which leads to a reduction in such polarization charges. Thus we expect that at higher volume fractions, the polarization charges arising from the other particles and its interactions are also likely to become screened. Together, such multibody effects reduce the influence of polarization and makes the inhomogeneous dielectric system more similar to the homogeneous system.

To summarize, the results discussed above demonstrate that the effect of dielectric inhomogeneity between the particle and the solvent reduces with increase in particle volume fraction.

4.1.3 Effect of the particle charge. In Fig. 3(a), we display the effect of particle charge on the particle–particle RDF (for a fixed volume fraction $\phi_p = 0.188$ and counterion valency $z_{ion} = 3$). For both homogeneous and inhomogeneous cases, the RDF peak is seen to reduce with increase in particle charge (Fig. 3(a)). This result can be anticipated due to the increase in electrostatic

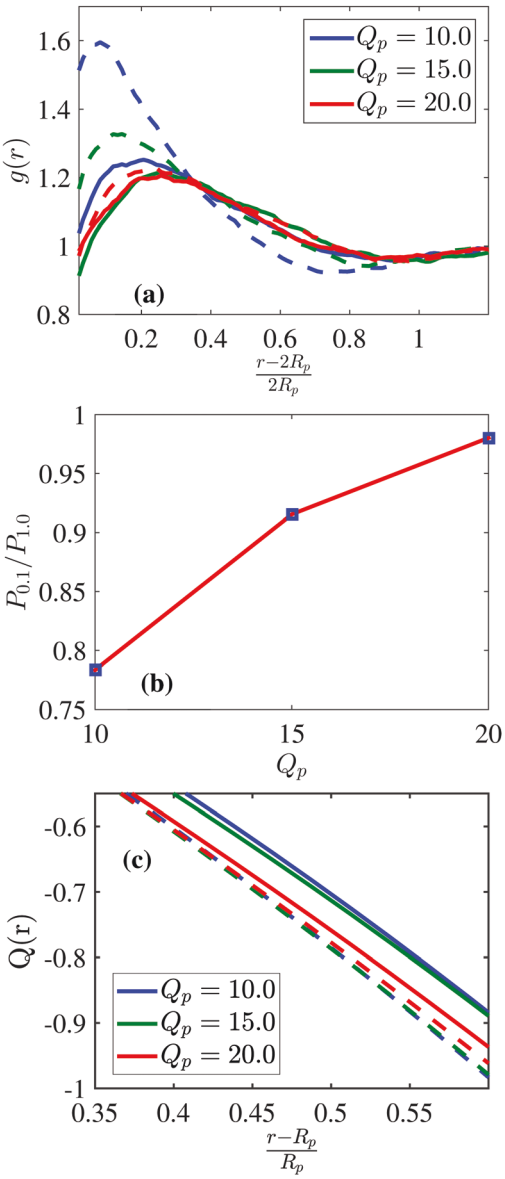

Fig. 3 (a) Particle–particle RDF at different dielectric constant cases at $\phi_p = 0.188$, counterion valency $z_{ion} = 3$ for different net charge of the particle; (b) ratio of peaks for RDF denoted by P_1 and $P_{0.1}$ for $\varepsilon_p/\varepsilon_w = 1.0$ and $\varepsilon_p/\varepsilon_w = 0.1$ respectively. The line represents a guide to the eye. (c) Average net charge around particle. The dashed lines represent result for $\varepsilon_p/\varepsilon_w = 1.0$. Solid lines represent result for $\varepsilon_p/\varepsilon_w = 0.1$.

repulsion between the particles arising from the increase in the bare charge. Further, consistent with the results discussed in the preceding sections, there is seen to be a lower peak for the inhomogeneous dielectric case relative to the homogeneous cases. More interestingly, the ratio of peak values of particle–particle RDF (comparing the homogeneous to inhomogeneous dielectric constant) is seen to increase with increase in charge of the particle as shown in Fig. 3(b).

To rationalize the interplay of particle charge and dielectric inhomogeneity, we again display in Fig. 3(c) the average net charge of counterions $Q(r)$ (normalized by the particle charge Q_p). Consistent with the results observed in $g(r)$, the differences

between the homogeneous and inhomogeneous dielectric systems are seen to decrease with an increase in the charge of the particle. We rationalize such results by invoking two aspects. First, we note that for higher charges of the particle, the interactions arising from the polarized charges as expected to become less important compared to the interaction due to bare counterion and particle charges. Indeed, as seen in eqn (19), at higher charge of the particle, the first term scales as $Q_p q$ and is expected to dominate the second term which scales as q^2. A second factor influencing the results is that, at higher net charge of the particle, there is expected to be more counterions present around the particle. Due to the screening of the induced charges arising from counterions located symmetrically with respect to the particle center, there is expected to be a cancellation in the polarization effects as seen in eqn (21). We note that the above results are consistent with previous studies on similar systems which show analytically the effect of surface polarization decreases with increase in particle charge.[17,40]

In summary, for System I, the inhomogeneities in dielectric contrast are seen to increase the repulsive particle–particle interactions and reduce the peak of the radial distribution function. The effect of particle and solvent dielectric contrast were observed to become more prominent at high counterion valencies. However, the effect of the dielectric contrast was seen to become mitigated with increase in particle volume fractions and/or charge of the particle.

4.2 Structural characteristics of System II

In this section, we discuss the results for the system of charged nanoparticles in presence of uncharged polymer solution and counterions. In this case, the direct interparticle interactions are modeled as simple excluded volume interactions. However, the presence of polymer is expected to lead to an effective attraction between the particles termed as the depletion interaction.[41–47] The characteristics of such depletion interactions for the case of uncharged particles and uncharged polymers have been well studied and is known to be purely attractive with the strength dependent on the concentration of polymer.[48–50] As we discuss below, a novel aspect of the present study is that the contrast between dielectric constant of the polymers and the solvent (in addition to that of the particle) may also be expected to affect the physics of the resulting depletion interactions.

In this section, we study the interplay of multibody effects on depletion interactions (arising due to polymers) with electrostatic interactions arising due to presence of charged particles. Specifically, our objective here is to quantify the influence of inhomogeneity in dielectric constant on such interactions and the equilibrium structural characteristics of the particles.

4.2.1 Effect of polymer dielectric contrast on depletion interactions. To elaborate on the influence of the contrast between dielectric constant of the polymers and the solvent (in addition to that of the particle) upon the effective depletion interactions, we consider the specific contribution of dielectric contrast to the potential field acting on the polymer monomers in our SCMF simulations:

$$\begin{aligned}\beta w_{\mathrm{pol}} &= -\frac{\partial \varepsilon}{\partial \rho_{\mathrm{pol}}}\frac{1}{8\pi l_{\mathrm{b}}\varepsilon_{\mathrm{w}}}|\nabla\varphi(\mathbf{r})|^2 \\ &= \left(1-\frac{\varepsilon_{\mathrm{poly}}}{\varepsilon_{\mathrm{w}}}\right)\frac{1}{8\pi l_{\mathrm{b}} C^{**}\varepsilon_{\mathrm{w}}}|\nabla\varphi(\mathbf{r})|^2.\end{aligned} \tag{23}$$

From eqn (23), it is evident that even if the polymer is uncharged, the equilibrium concentration of polymers is expected to be affected by the electric field due to the dependence of dielectric constant of the medium on the density of polymer (*i.e.* the term $(\partial\varepsilon/\partial\rho_{\mathrm{pol}})$). For the specific model of mixture dielectric constant (eqn (14)) adopted in this work, the last term in the field expression (eqn (23)) is seen to depend on the value of $\varepsilon_{\mathrm{pol}}/\varepsilon_{\mathrm{w}}$. More explicitly, for $\varepsilon_{\mathrm{pol}}/\varepsilon_{\mathrm{w}} < 1$, there is expected to be an "enhanced depletion" of polymers relative to the homogeneous dielectric cases. As a consequence, there is also expected to be an increased depletion attraction induced between the particles. In contrast, when $\varepsilon_{\mathrm{pol}}/\varepsilon_{\mathrm{w}} > 1$, there is expected to be an "adsorption" of polymers relative to the homogeneous dielectric cases, and concomitantly, a reduction in the depletion attraction induced between the particles.

To demonstrate the validity of the above arguments, we considered the case of a single charged particle in a polymer solution at a fixed polymer concentration for different dielectric constant of the polymer, and display the resulting polymer concentration profiles in Fig. 4(a).

From the results, it is evident that the polymer exhibit reduced depletion for $\varepsilon_{\mathrm{pol}}/\varepsilon_{\mathrm{w}} > 1$ and an enhanced depletion for $\varepsilon_{\mathrm{pol}}/\varepsilon_{\mathrm{w}} < 1$. More pertinently, the results for $\varepsilon_{\mathrm{pol}}/\varepsilon_{\mathrm{w}} = 1$ are seen to be independent of the value of $\varepsilon_{\mathrm{p}}/\varepsilon_{\mathrm{w}}$, demonstrating that the polymer concentrations are not influenced by the dielectric contrast between the particle and solvent for such cases.

While the above results relate to single particle system, a more pertinent question is the influence of such effects in multiparticle systems. With regards to multiparticle systems (at a fixed particle volume fraction $\phi_{\mathrm{p}} = 0.188$ and particle charge $Q_{\mathrm{p}} = 15$), we first consider the influence of $\varepsilon_{\mathrm{p}}/\varepsilon_{\mathrm{w}}$ on the polymer depletion effects of Fig. 4(b) and (c). In comparing the case where $\varepsilon_{\mathrm{p}}/\varepsilon_{\mathrm{w}} < 1$ and $\varepsilon_{\mathrm{p}}/\varepsilon_{\mathrm{w}} = 1$, we observe that the RDFs (Fig. 4(b)) for the case of $\varepsilon_{\mathrm{p}}/\varepsilon_{\mathrm{w}} = 1$ exhibit much stronger peaks compared to the system in which $\varepsilon_{\mathrm{p}}/\varepsilon_{\mathrm{w}} < 1$. Correspondingly, in Fig. 4(c) we observe that the polymer concentrations exhibit higher local concentrations (reduced depletion) for the situation with particle–solvent dielectric contrast. To rationalize the results for polymer concentration, we note that in general, the presence of a third particle in the vicinity of two particles is expected to reduce the local polymer concentrations ("multibody" effect on depletion). However, in situation where there is particle–solvent dielectric contrast, there is an enhanced repulsive interaction between particles (Section 4.1). As a consequence, particles are on an average farther apart. Such an enhanced interparticle separation is expected to reduced "multibody" effect of depletion and thereby increase the local polymer concentrations.[11,51,52]

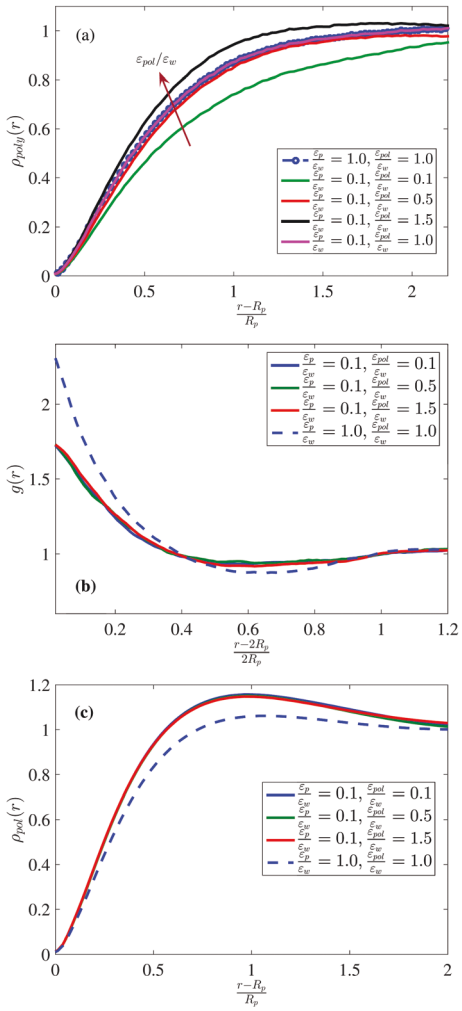

Fig. 4 (a) Polymer concentration profile around a particle of charge Q_p = 10, the bulk polymer concentration C/C^* = 0.09 and counterion valency z_{ion} = 3. (b) Particle–particle RDF in a multiparticle system with charge Q_p = 15, particle volume fraction ϕ_p = 0.188, bulk polymer concentration C/C^* = 0.09, counterion valency z_{ion} = 3. (c) Polymer concentration around a particle in a multiparticle system with charge Q_p = 15, particle volume fraction ϕ_p = 0.188, bulk polymer concentration C/C^* = 0.09, counterion valency z_{ion} = 3.

In a previous study from our group, Pandav *et al.* probed the interplay between particle volume fractions and the polymer-induced depletion interactions within a canonical ensemble framework of a fixed concentration of polymers. In such a framework, they showed that an increase in particle volume fraction while maintaining a fixed concentration of polymer is equivalent to increasing the chemical potential of the polymer, and thereby leads to an increase in the strength of attractive depletion interactions. Our above results demonstrate that in the presence of dielectric contrast between the particle and solvent, such multibody depletion effects are expected to become reduced. As a consequence, system with particle–solvent dielectric contrast are expected to demonstrate weaker depletion interactions relative to the homogeneous system. Such a reasoning explains the results observed in the particle–particle RDF shown in Fig. 4(b).

In examining the influence of polymer–solvent dielectric contrast for the finite particle volume fraction, from Fig. 4(b) and (c), we observe that the results for the particle structure and polymer concentration are insensitive to the dielectric contrast between the polymer and the solvent. These results are in contrast to the trends discussed in Fig. 4(a). We rationalize such results by invoking that at higher particle concentrations the electrostatic potential is expected to be screened, thereby reducing the effects of the contribution of eqn (23). Surprisingly, we observe that for even a low particle volume fraction of ϕ_p = 0.18, suffices to render the influence of $\varepsilon_{pol}/\varepsilon_w$ irrelevant. Together, the above results suggest that while at the one particle level the polymer depletion is indeed affected by the dielectric contrast between the polymer and the solvent, at finite particle concentration, the influence of the contrast between the polymer and solvent dielectric constant proves less relevant. More pertinently, we observe that the particle–solvent dielectric contrast serves to mitigate the multibody effects on depletion and thereby reduce the effective polymer-induced attraction between the particles.

For the rest of the article we do not probe the effects of $\varepsilon_{pol}/\varepsilon_w$ and instead set $\varepsilon_{pol}/\varepsilon_w$ = 0.1. We present the results for the effect of particle volume fraction, polymer concentration and particle charge on the equilibrium structure behavior.

4.2.2 Effect of polymer concentration. Fig. 5 displays the influence of polymer concentration on the particle–particle RDFs at a fixed particle volume fraction of ϕ_p = 0.188 and particle charge Q_p = 10. In general, the particle–particle RDFs are seen to exhibit a sharper peak in System II when compared to the results for System I (Fig. 1(a)). Such results can be rationalized as a consequence of the shorter ranged nature of the depletion interaction compared to the LJ interactions modeled in System I. For both homogeneous and inhomogeneous particle dielectric situations, the peak of particle–particle radial distribution function in Fig. 5(a) is seen to increase with increase in concentration of polymer. Such observations can be straightforwardly understood as a consequence of the increased depletion attractions manifesting in more concentrated polymer solutions. To quantify explicitly the influence of dielectric contrast between the particle and the solvent, we again display the ratio of peaks of particle–particle RDF represented by $P_{0.1}/P_{1.0}$ (Fig. 5(b)). It is seen that $P_{0.1}/P_{1.0}$ decreases with increase in polymer concentration, suggesting that the influence of inhomogeneity in dielectric constant becomes more prominent with increase in polymer concentration.

To rationalize the above results, we note that in systems with dielectric contrast, the electrostatic repulsion is expected to be stronger relative to the case of homogeneous dielectric constant. As a consequence the particles are expected to be present in more proximity for the homogeneous dielectric system. When such a factor is coupled with the multibody effects on "depletion" discussed in the previous section, we expect the local polymer concentrations to be higher for the inhomogeneous dielectric system. This expectation is confirmed in the results shown in Fig. 5(c) and more explicitly in the ratio of peaks of the concentration shown in Fig. 5(d). As a result there

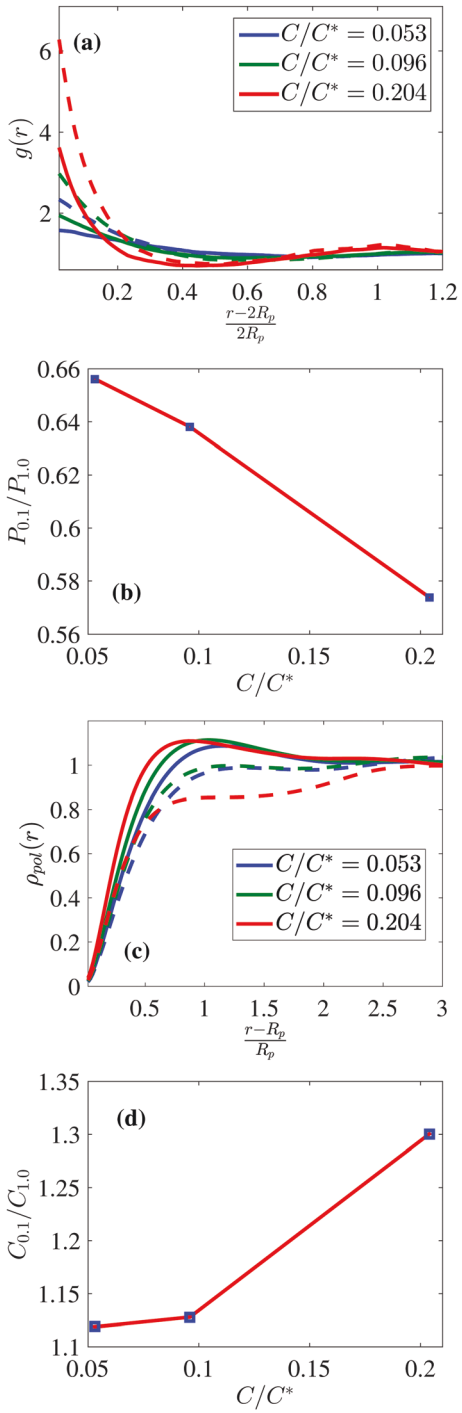

Fig. 5 (a) Particle–particle RDF for particles with charge $Q_p = 10$, particle volume fraction $\phi_p = 0.188$, counterion valency $z_{ion} = 3$; (b) ratio of peaks of particle–particle RDF for $\varepsilon_p/\varepsilon_w = 1$ and $\varepsilon_p/\varepsilon_w = 0.1$; the line represents a guide to the eye. (c) Normalized polymer concentration profile around a particle. (d) Ratio of peak of polymer concentration profile for $\varepsilon_p/\varepsilon_w = 1$ and $\varepsilon_p/\varepsilon_w = 0.1$. The line represents a guide to the eye. The dashed lines represent the RDF for $\varepsilon_p/\varepsilon_w = 1$. The solid lines represent that when $\varepsilon_p/\varepsilon_w = 0.1$.

is a reduction in the effective "depletion" interactions for the inhomogeneous dielectric system and such differences between the homogeneous and inhomogeneous systems increases with increase in polymer concentration. Such an effect can be hypothesized to be responsible for the decrease in the ratio of $P_{0.1}/P_{1.0}$ with polymer concentration.

To summarize, with an increase in polymer concentration, the influence of dielectric inhomogeneity on the particle structure is seen to increase. We argued that such results arise as a consequence of an interplay of electrostatics and the multibody effects in depletion interactions.

4.2.3 Effect of particle volume fraction. Fig. 6(a) displays the interplay of polymer depletion and electrostatic interaction on the particle–particle RDF for different particle volume fractions at a fixed bulk polymer concentration $C/C^* = 0.096$ and particle charge $Q_p = 10$. With increase in particle volume fraction, the peak of the RDF is seen to increase for both homogeneous and inhomogeneous dielectric cases, signaling an increase in the effective interparticle attraction. As discussed before, such a result is consistent with both the enhanced screening of electrostatics and increased depletion attraction expected for multiparticle systems. More pertinently, the RDF for the inhomogeneous dielectric constant is seen to be lower than the corresponding homogeneous dielectric system. Explicitly, the ratio of the RDF peak values for inhomogeneous to homogeneous case, $P_{0.1}/P_1$, increases with increase in particle volume fraction (Fig. 6(b)). While the trends in System II mirror those seen in System I, the values of the ratio of $P_{0.1}/P_{1.0}$ are seen to be always lower than those in System I. Such results indicate enhanced repulsion (comparing the homogeneous and inhomogeneous dielectric case) in polymer solutions.

Similar to the results discussed in Section 4.1.2, the effect of particle volume fraction on $P_{0.1}/P_{1.0}$ (for both System I and II) can be understood as a consequence of the screening of electrostatic field in systems. To rationalize the depletion effects and the differences between system I and II, we again invoke the influence of dielectric inhomogeneity on the polymer-induced depletion interactions. Towards this objective, in Fig. 6(c), we display the average polymer concentration around the particle for different particle volume fractions. For inhomogeneous dielectric system, the polymer concentration profiles are seen to be more closer to the particle when compared to the homogeneous dielectric system. These trends are in line with the results discussed in the context of Fig. 5(b), and is consistent with the reduced depletion for inhomogeneous dielectric systems. More particularly, the differences between the polymer concentration profiles for the homogeneous and inhomogeneous dielectric system, as quantified by the ratio of peaks of polymer concentration profiles, $C_{0.1}/C_{1.0}$, decreases with increase in volume fraction of the particles (Fig. 6(d)). To understand these results, we note that at higher particle volume fraction, due to the screening effects, the electrostatic interactions and the structural differences arising as a consequence between homogeneous and inhomogeneous dielectric systems become reduced. As a result, the differences in the "multibody" depletion effects between such systems also become reduced, leading to similar polymer concentration profiles and depletion interaction for the homogeneous and inhomogeneous dielectric systems.

In general in System II, the particle–solvent dielectric inhomogeneity leads to two sources which contribute to repulsive

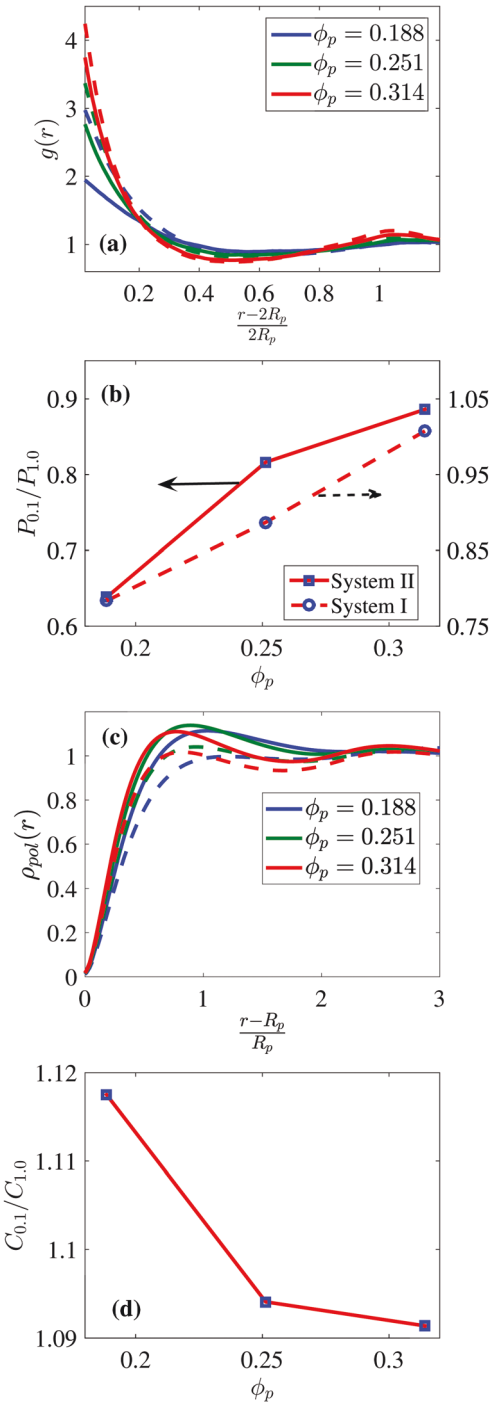

Fig. 6 (a) Particle–particle RDF for particles with charge Q_p = 10, bulk polymer concentration C/C^* = 0.09, counterion valency z_{ion} = 3; (b) ratio of the peaks of particle–particle RDF for $\varepsilon_p/\varepsilon_w$ = 1 and $\varepsilon_p/\varepsilon_w$ = 0.1; the line represents a guide to the eye. (c) Normalized polymer concentration profile around the particle. (d) Ratio of peak for polymer concentration profile for $\varepsilon_p/\varepsilon_w$ = 1 and $\varepsilon_p/\varepsilon_w$ = 0.1. The line represents a guide to the eye. The dashed lines represent results for $\varepsilon_p/\varepsilon_w$ = 1.0 and solid lines represent results for $\varepsilon_p/\varepsilon_w$ = 0.1 respectively.

interactions between the charged particles: the first is the effect on the electrostatic interactions through polarization, and the second, arising from the multibody effects on the reduced depletion interaction. Our above results suggest that the second effect becomes mitigated at higher particle volume fractions, and hence the systems with dielectric inhomogeneity become more similar to the homogeneous system. Thus the ratio $P_{0.1}/P_{1.0}$ increases at a faster rate for System II.

Together, the results discussed above demonstrate that with increase in particle volume fraction, the influence of particle dielectric inhomogeneity decreases. Compared to System I, due to the interplay of multibody effect of electrostatic and depletion interaction, the influence of dielectric inhomogeneity is more prominent in System II, and is manifested in terms of lower value of $P_{0.1}/P_{1.0}$ especially at lower particle volume fractions. However, in System II, the polymer-induced interactions also exhibit less sensitivity to particle–solvent dielectric contrast at higher volume fractions. This effect is manifested by the faster rate at which the ratio vary with ϕ_p in System II as compared to System I.

4.2.4 Effect of particle charge. Fig. 7(a) displays the effect of particle charge on the radial distribution function of charged particles in polymer solution at a constant bulk polymer concentration C/C^* = 0.09 and particle volume fraction ϕ_p = 0.188. For all cases, with increase in particle charge, the intensity of the peak in RDF is seen to decrease, indicating weakened aggregation. This is expected, due to the increased electrostatic repulsion arising as a consequence of increased charge of the particle. The ratio of peak of the particle–particle RDF for the homogeneous and inhomogeneous cases are shown in Fig. 7(b). For the inhomogeneous dielectric constant cases, the RDF peaks are seen to be lesser than the respective homogeneous system, and the ratio $P_{0.1}/P_{1.0}$ is seen to increase with increase in net charge of the particle. Interestingly, the values for the ratio $(P_{0.1}/P_{1.0})$ for all values of Q_p are seen to be lower for System II in comparison to System I.

To understand the differences between System I and II, in Fig. 7(c), we display the polymer concentration around the particle as a function of the net particle charge. For both homogeneous and inhomogeneous systems, with increase in particle net charge Q_p, the peak of the polymer concentration profiles are seen to increase. To rationalize this observation, we note that with increase in charge, the particles are expected to be more separated due to electrostatic repulsion. As discussed in the previous section, when particles are more dispersed, the multibody effects on polymer depletion (which results in more polymers near a particle) is expected to reduce. More interestingly, the differences in such multibody effects, quantified by the ratio $C_{0.1}/C_{1.0}$ (Fig. 7(d)) is seen to decrease with increase in net charge of the particle. This observation can be understood by the fact that at higher net charge of the particle, the effect of polarized charges become less important, and hence the electrostatic effects on the particle structure becomes very similar for homogeneous and inhomogeneous systems. As a consequence, the differences in multibody effects on depletion between homogeneous and inhomogeneous dielectric systems are also expected to become smaller with increase in particle charges. Similar to the effects discussed in the previous section, such trends can be expected to lead to a faster rise in $P_{0.1}/P_{1.0}$ with particle charge Q_p.

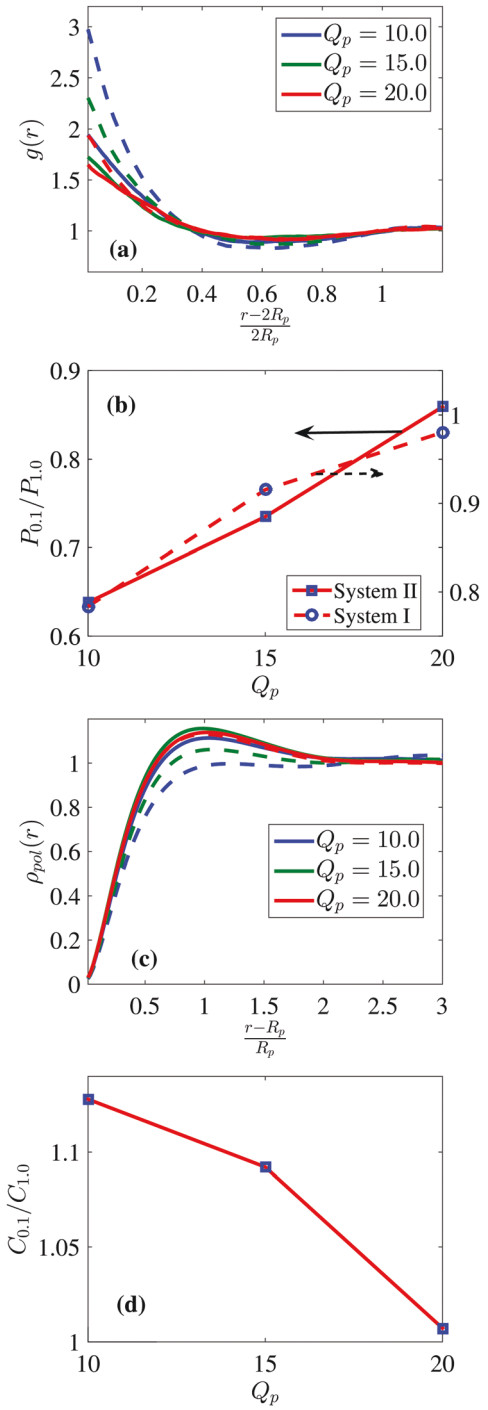

Fig. 7 (a) Particle–particle RDF with particle volume fraction ϕ_p = 0.188, bulk polymer concentration C/C^* = 0.09, counterion valency z_{ion} = 3; (b) ratio of RDF peaks for $\varepsilon_p/\varepsilon_w$ = 1 and $\varepsilon_p/\varepsilon_w$ = 0.1 respectively; the line represents a guide to the eye. (c) Normalized polymer concentration profile around the particle; (d) ratio of peak for polymer concentration profile for $\varepsilon_p/\varepsilon_w$ = 1 and $\varepsilon_p/\varepsilon_w$ = 0.1 respectively. The line represents a guide to the eye. The solid lines represent the result for homogenous dielectric system. The dashed lines represent result for $\varepsilon_p/\varepsilon_w$ = 0.1.

To summarize, with increase in particle net charge, the influence of dielectric inhomogeneity on the particle structure reduces. We argued that such results are due to decrease in polarized charges and the decrease in the multibody effects of depletion interaction with increase in the net particle charge. Compared to System I, due to the interplay of multibody effect of electrostatic and depletion interaction, the influence of dielectric inhomogeneity is more prominent in System II manifested in terms of lower value of $P_{0.1}/P_{1.0}$ and higher rate at which the ratio vary with Q_p as compared to System I.

5 Conclusions

In this article we have presented results for the application of SCMF simulation framework on a system of charged nanoparticles in presence of uncharged polymer solution, and studied the effect of dielectric contrast between particles and solvent. We have considered two related systems: System I in which we considered charged particles interacting by LJ interactions; and System II where we considered charged particles in uncharged polymer solution. For both systems, we studied the influence of particle volume fraction, charge of the particle, counterion valency and polymer concentration (System II) on the equilibrium structure of particles.

For System I, it was seen that the effect of particle dielectric contrast becomes significant at higher counterion valency. With increase in particle volume fraction and net charge, the effect of dielectric inhomogeneity was seen to become reduced. For System II, in the case of a single particle, with increase in dielectric constant of the polymer with respect to the solvent the depletion of polymer around the particle decreased. However, for the multiparticle systems, the dielectric constant of the polymer did not have a significant effect on the structural properties of particle or polymers. The influence of dielectric contrast between particle and solvent became important with increase in polymer concentration and decrease in particle volume fraction and particle net charge. Compared to System I, due to the interplay of multibody effect of electrostatic and depletion interaction, the influence of inhomogeneity in dielectric contrast was found to be more prominent for System II.

Conflicts of interest

There are no conflicts to declare.

Acknowledgements

We are grateful to Dr Jian Qin, Dr Issei Nakamura and Dr Victor Pryamitsyn for their valuable comments on a preprint of this article. We acknowledge funding in part by grants from the Robert A. Welch Foundation (Grant F1599), the National Science Foundation (DMR-1721512), to King Abdullah University of Science and Technology (OSR-2016-CRG5-2993-1). Acknowledgment is also made to the Donors of the American Chemical Society Petroleum Research Fund for partial support of this research (56715-ND9). We acknowledge the Texas Advanced Computing Center (TACC) at The University of Texas at Austin

for computing resources that contributed to the research results reported within this paper.

References

1 M. R. Roy Shenhar and T. B. Norsten, *Adv. Mater.*, 2005, **17**, 657–669.
2 K. P. Johnston, J. A. Maynard, T. M. Truskett, A. U. Borwankar, M. A. Miller, B. K. Wilson, A. K. Dinin, T. A. Khan and K. J. Kaczorowski, *ACS Nano*, 2012, **6**, 1357–1369.
3 R. Stover, A. K. Murthy, G. D. Nie, S. Gourisankar, B. J. Dear, T. Truskett, K. V. Sokolov and K. P. Johnston, *Quenched Assembly of NIR-Active Gold Nanoclusters Capped with Strongly Bound Ligands by Tuning Particle Charge via pH and Salinity*, 2014.
4 A. K. Murthy, R. J. Stover, A. U. Borwankar, G. D. Nie, S. Gourisankar, T. M. Truskett, K. V. Sokolov and K. P. Johnston, *ACS Nano*, 2013, **7**, 239–251.
5 E. Dickinson and L. Eriksson, *Adv. Colloid Interface Sci.*, 1991, **34**, 1–29.
6 E. Dickinson, *Soft Matter*, 2006, **2**, 642–652.
7 J. Gregory and S. Barany, *Adv. Colloid Interface Sci.*, 2011, **169**, 1–12.
8 W. B. Russel, D. A. Saville and W. R. Schowalter, *Colloidal dispersions*, Cambridge University Press, 1989, vol. 54, pp. 201–202.
9 F. Carlsson, P. Linse and M. Malmsten, *J. Phys. Chem. B*, 2001, **105**, 9040–9049.
10 M. Skepö and P. Linse, *Phys. Rev. E: Stat., Nonlinear, Soft Matter Phys.*, 2002, **66**, 051807.
11 G. Pandav, V. Pryamitsyn and V. Ganesan, *Langmuir*, 2015, **31**, 12328–12338.
12 E. Kizilay, A. B. Kayitmazer and P. L. Dubin, *Adv. Colloid Interface Sci.*, 2011, **167**, 24–37.
13 J.-P. Hansen and H. Löwen, *Annu. Rev. Phys. Chem.*, 2000, **51**, 209–242.
14 J. D. Jackson, *Classical Electrodynamics*, Wiley, 1999.
15 J. A. Stratton, *Electromagnetic Theory*, 1941.
16 P. Linse, *J. Chem. Phys.*, 2008, **128**, 214505.
17 R. Messina, *J. Chem. Phys.*, 2002, **117**, 11062–11074.
18 K. Barros and E. Luijten, *Phys. Rev. Lett.*, 2014, **113**, 017801.
19 J. Qin, J. Li, V. Lee, H. Jaeger, J. J. de Pablo and K. F. Freed, *J. Colloid Interface Sci.*, 2016, **469**, 237–241.
20 M. C. Barbosa, M. Deserno, C. Holm and R. Messina, *Phys. Rev. E: Stat., Nonlinear, Soft Matter Phys.*, 2004, **69**, 051401.
21 R. Messina, *Phys. Rev. E: Stat., Nonlinear, Soft Matter Phys.*, 2004, **70**, 051802.
22 P. Linse and L. Lue, *J. Chem. Phys.*, 2014, **140**, 044903.
23 M. Seijo, M. Pohl, S. Ulrich and S. Stoll, *J. Chem. Phys.*, 2009, **131**, 174704.
24 A. P. dos Santos, A. Bakhshandeh and Y. Levin, *J. Chem. Phys.*, 2011, **135**, 044124.
25 L. Lue and P. Linse, *J. Chem. Phys.*, 2015, **142**, 144902.
26 J. Rescic and P. Linse, *J. Chem. Phys.*, 2008, **129**, 114505.
27 V. Pryamitsyn and V. Ganesan, *Macromolecules*, 2014, **47**, 6095–6112.
28 V. Pryamitsyn and V. Ganesan, *J. Chem. Phys.*, 2015, **143**, 164904.
29 H. Lian and J. Qin, *Mol. Syst. Des. Eng.*, 2018, **3**, 197–203.
30 J. Qin, J. J. de Pablo and K. F. Freed, *J. Chem. Phys.*, 2016, **145**, 124903.
31 M. Doi and S. Edwards, *The Theory of Polymer Dynamics*, A Clarendon Press Publication, 1988.
32 G. H. Fredrickson, *The equillibrium theory of inhomogenous polymers*, Oxford Science Publications, 2006.
33 K. C. Daoulas and M. Müller, *J. Chem. Phys.*, 2006, **125**, 184904.
34 A. Levy, D. Andelman and H. Orland, *Phys. Rev. Lett.*, 2012, **108**, 227801.
35 X. Duan and I. Nakamura, *Soft Matter*, 2015, **11**, 3566–3571.
36 A. Levy, D. Andelman and H. Orland, *J. Chem. Phys.*, 2013, **139**, 164909.
37 N. Metropolis, A. W. Rosenbluth, M. N. Rosenbluth, A. H. Teller and E. Teller, *J. Chem. Phys.*, 1953, **21**, 1087–1092.
38 K. S. Gustafson, G. Xu, K. F. Freed and J. Qin, *J. Chem. Phys.*, 2017, **147**, 064908.
39 S. Alexander, P. M. Chaikin, P. Grant, G. J. Morales, P. Pincus and D. Hone, *J. Chem. Phys.*, 1984, **80**, 5776–5781.
40 P. Linse, *J. Phys. Chem.*, 1986, **90**, 6821–6828.
41 P. G. Bolhuis and A. A. Louis, *Macromolecules*, 2002, **35**, 1860–1869.
42 M. Robins and A. Fillery-Travis, *J. Chem. Technol. Biotechnol.*, 1992, **54**, 201–202.
43 A. P. Chatterjee and K. S. Schweizer, *J. Chem. Phys.*, 1998, **109**, 10464–10476.
44 R. Tuinier, G. A. Vliegenthart and H. N. W. Lekkerkerker, *J. Chem. Phys.*, 2000, **113**, 10768–10775.
45 P. G. Bolhuis, A. A. Louis, J. P. Hansen and E. J. Meijer, *J. Chem. Phys.*, 2001, **114**, 4296–4311.
46 A. A. Louis, P. G. Bolhuis, E. J. Meijer and J. P. Hansen, *J. Chem. Phys.*, 2002, **117**, 1893–1907.
47 R. Tuinier, J. Rieger and C. de Kruif, *Adv. Colloid Interface Sci.*, 2003, **103**, 1–31.
48 S. Asakura and F. Oosawa, *J. Chem. Phys.*, 1954, **22**, 1255–1256.
49 S. Asakura and F. Oosawa, *J. Polym. Sci.*, 1958, **33**, 183–192.
50 V. Pryamitsyn and V. Ganesan, *J. Chem. Phys.*, 2013, **138**, 234905.
51 M. Surve, V. Pryamitsyn and V. Ganesan, *J. Chem. Phys.*, 2005, **122**, 154901.
52 E. J. Meijer and D. Frenkel, *Phys. Rev. Lett.*, 1991, **67**, 1110–1113.